

Hiroshi Yoshihara\* and Masahiro Yoshinobu

# Young's modulus and shear modulus of solid wood measured by the flexural vibration test of specimens with large height/length ratios

**Abstract:** The Young's modulus (modulus of elasticity, MOE) in the longitudinal (L) and radial (R) directions and the shear modulus (SM) in the LR plane of Douglas fir were determined by the flexural vibration (FV) tests under the free-free condition based on Timoshenko's vibration equation. In the tests, the height/length ( $H/L$ ) ratio was varied from 0.05 to 0.3. In addition, the test data were analyzed numerically and the effectiveness of Timoshenko's equation was examined. The MOE and SM were calculated based on the rigorous and approximated solutions of Timoshenko's equation. The inaccuracy of the approximated solution was enhanced when the  $H/L$  ratio of the specimen was too large. In contrast, the rigorous solution enabled the accurate calculation of these moduli in a wider range of length/depth ratios than the approximated solution.

**Keywords:** finite element analysis (FEA), flexural vibration (FV) test, height/length ratio of specimens, shear modulus (SM), Timoshenko's vibration equation, Young's modulus (MOE)

DOI 10.1515/hf-2014-0151

Received May 19, 2014; accepted September 22, 2014; previously published online October 18, 2014

## Introduction

The flexural vibration (FV) method is advantageous because the Young's modulus (modulus of elasticity, MOE) and shear modulus (SM) can be obtained simultaneously from a single specimen. To determine these moduli, an approximate solution of Timoshenko's vibration equation according to Goens (1931) (T-G equation) has a high popularity because of its convenience (Hearmon 1958, 1966; Ono and Kataoka 1979a,b; Ono 1983; Nakao 1984; Sobue 1986; Chui and Smith 1990;

Kubojima et al. 1996, 1997; Divós et al. 1998; Brancheriau and Baillères 2002, 2003; Divós et al. 2005; Brancheriau 2006; Murata and Kanazawa 2007; Tonosaki et al. 2010; Sohi et al. 2011; Yoshihara 2012a,b; Kubojima and Tonosaki 2013). In the FV method, however, a specific specimen configuration is needed for accurate measurements. When the specimen is too slender, the shear deflection contribution is too small, and the  $SM_{in-plane}$  is often incorrect because minor errors in the resonance frequency determination lead to the inaccuracies (Kubojima et al. 1996, 1997). Thus, the specimen must have a large height relative to the length. Based on the approximate solution of the T-G equation, Kubojima et al. (1997) proposed an equation for determining the lowest bound of the height/length ( $H/L$ ) ratio that can reduce the inaccuracy of SM to a certain error level. Yoshihara (2012b) measured the MOE and SM values of solid Sitka spruce (*Picea sitchensis*) wood, plywood (Lauan, *Shorea* sp.), and medium-density fiberboard (MDF) with specimens having the  $H/L$  ratio between 0.033 and 0.2. In this range, the effect of  $H/L$  ratio of spruce specimens was small. In contrast, there is a concern that the vibrational behaviors of the specimen may deviate from that predicted by the T-G equation, when the  $H/L$  ratio is very large.

This is the reason why, in the present study, the free-free FV tests will be performed on specimens with a special configuration. The length direction of the sample coincides with the longitudinal (L) or radial (R) direction, while the specimens will have a varying  $H/L$  range between 0.05 and 0.3. The MOE and SM will be calculated by means of the rigorous Timoshenko's equation and by the simplified T-G equation. The validity of the solutions will be examined by comparing the results with those of finite element (FE) calculations.

## Theoretical considerations

### FV equations

Figure 1Aa shows a schematic of the specimen and the FE model. The specimens in which the length direction

\*Corresponding author: Hiroshi Yoshihara, Faculty of Science and Engineering, Shimane University, Nishikawazu-cho 1060, Matsue, Shimane 690-8504, Japan, e-mail: yoshihara@riko.shimane-u.ac.jp  
Masahiro Yoshinobu: Faculty of Science and Engineering, Shimane University, Nishikawazu-cho 1060, Matsue, Shimane 690-8504, Japan

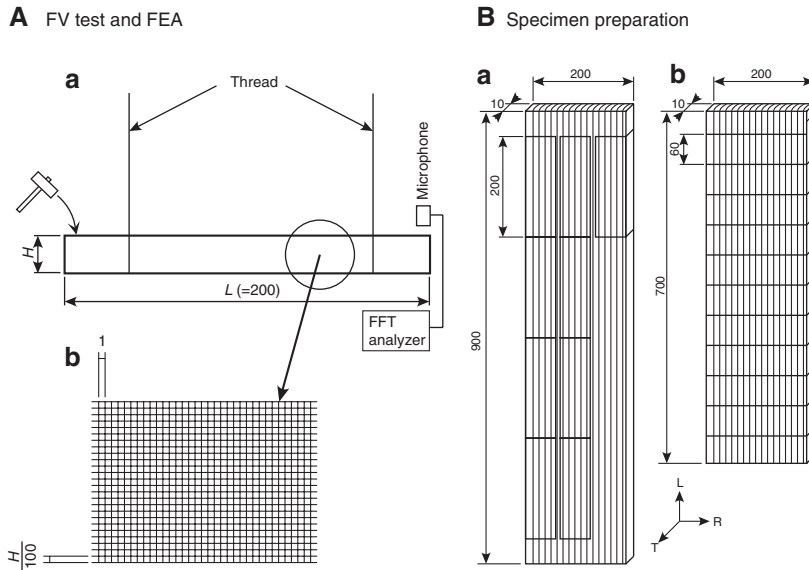


**Figure 1** (A) Schemes of the FV test (a) and the FEA of the FV data (b).  $H=10, 20, 30, 40, 50,$  and  $60$  mm. (B) Preparation of the specimens with the initial dimensions. (a) L-type and (b) R-type specimens (mm).

coincides with the L and R directions are designated correspondingly. In the L specimen, the orthotropic axes ( $x, y,$  and  $z$ ) coincide with the L, R, and tangential (T) directions, respectively. In the R specimen, the  $x, y,$  and  $z$  axes coincide with the R, L, and T directions, respectively. The MOE in the  $x$  direction is defined as  $E_x$ , and the SM in the  $xy$  plane is defined as  $G_{xy}$ .

Timoshenko (1921) developed the differential equation of flexure, in which the shear deflection and rotary inertia were taken into account in the free-free flexural condition as follows:

where  $L$  and  $H$  are the length and height of the specimen, respectively;  $\rho$  is the density; and  $s$  is Timoshenko's shear factor. The  $s$  value is usually affected by the configuration and elastic moduli of the specimen (Yoshihara 2012a,c). In this study, the  $s$  value is set as 1.2 for the specimen. When the resonance frequency for the  $n$ th FV mode is defined as  $f_n$ ,  $k_n$  is derived as follows:

$$k_n = \sqrt[4]{\frac{48\pi^2 \rho}{E_x H^2} L f_n} \quad (3)$$

$$\begin{cases} \frac{\tan \frac{k_n}{2} \sqrt{\beta^2 k_n^4 + 1 + \alpha k_n^2}}{\tanh \frac{k_n}{2} \sqrt{\beta^2 k_n^4 + 1 - \alpha k_n^2}} + \frac{\sqrt{\beta^2 k_n^4 + 1 + \alpha k_n^2}}{\sqrt{\beta^2 k_n^4 + 1 - \alpha k_n^2}} \cdot \frac{\sqrt{\beta^2 k_n^4 + 1 - \beta k_n^2}}{\sqrt{\beta^2 k_n^4 + 1 + \beta k_n^2}} = 0 & \text{(symmetric mode)} \\ \frac{\cot \frac{k_n}{2} \sqrt{\beta^2 k_n^4 + 1 + \alpha k_n^2}}{\coth \frac{k_n}{2} \sqrt{\beta^2 k_n^4 + 1 - \alpha k_n^2}} - \frac{\sqrt{\beta^2 k_n^4 + 1 + \alpha k_n^2}}{\sqrt{\beta^2 k_n^4 + 1 - \alpha k_n^2}} \cdot \frac{\sqrt{\beta^2 k_n^4 + 1 - \beta k_n^2}}{\sqrt{\beta^2 k_n^4 + 1 + \beta k_n^2}} = 0 & \text{(anti-symmetric mode)} \end{cases} \quad (1)$$

$$\begin{cases} \alpha = \frac{1}{24} \left( \frac{H}{L} \right)^2 \left( \frac{s E_x}{G_{xy}} + 1 \right) \\ \beta = \frac{1}{24} \left( \frac{H}{L} \right)^2 \left( \frac{s E_x}{G_{xy}} - 1 \right) \end{cases} \quad (2)$$

The values of  $E_x$  and  $G_{xy}$  corresponding to each resonance mode can be simultaneously obtained from the numerical analysis based on Eq. (1). There are several examples for calculating the  $E_x$  and  $G_{xy}$  values by Eq. (1) (Mead and Joannides 1991; Kubojima et al. 1996, 1997; Yoshihara 2012a,b,c).

In addition to the rigorous solution, Goens (1931) also derived an approximate solution of Timoshenko's equation (T-G equation):

$$\frac{m_n^4}{k_n^4} = 1 + \frac{m_n F(m_n)}{6} \left( \frac{H}{L} \right)^2 \left( 3 - \frac{sE_x}{G_{xy}} \right) + \frac{m_n^2 F^2(m_n)}{12} \left( \frac{H}{L} \right)^2 \left( 1 + \frac{sE_x}{G_{xy}} \right) - \frac{\pi^2 s \rho H^2 f_n^2}{3G_{xy}} \quad (4)$$

The coefficients  $m_n$  and  $F(m_n)$ , which correspond to each resonance mode, are given by

$$m_1 = 4.730; m_2 = 7.853; m_n = [(2n+1)\pi] / 2, n \geq 3 \quad (5)$$

and

$$F(m_1) = 0.9825; F(m_2) = 1.0008; F(m_n) = 1, n \geq 3 \quad (6)$$

Hearmon (1958) proposed an iterative method, in which Eq. (4) is separated into  $X$  and  $Y$ :

$$\begin{cases} X = \frac{4\pi^2 \rho L^2 f_n^2}{m_n^4} \left[ -2m_n F(m_n) + m_n^2 F^2(m_n) \right] \\ Y = \frac{4\pi^2 \rho L^2 f_n^2}{m_n^4} \left[ 12 \left( \frac{L}{H} \right)^2 + 6m_n F(m_n) + m_n^2 F^2(m_n) - \frac{4\pi^2 s L^2 \rho f_n^2}{G_{xy}} \right] \end{cases} \quad (7)$$

The  $X$ - $Y$  relation corresponding to each mode is regressed into the linear function  $Y = q - pX$ , and the  $E_x$  and  $G_{xy}$  values are determined by the value of  $q$  and  $sq/p$ , respectively. The Hearmon's iteration method can be conducted easier than that based on the Goens' rigorous solution based on Eq. (1). Therefore, there are many possibilities for measuring the  $E_x$  and  $G_{xy}$  values of solid wood obtained by Eq. (7).

The T-G approach [Eq. (4)] is based on the concept that the material can be regarded as quasi-isotropic, such as the value of  $3-sE_x/G_{xy}$ , contained in the second term of the right side of the equation, which is in the range of  $-0.6$ – $0.1$ . Nevertheless, it is unclear whether this approximation is valid for the highly orthotropic materials such as solid wood. For example, the value of  $3-sE_x/G_{xy}$  of spruce is approximately  $-25$  when the length direction of the specimen coincides with the L direction (Ono and Kataoka 1979a,b). In addition, the influence of the second term in Eq. (4) is enhanced significantly when the  $H/L$  value increases. Therefore, it is doubtful that the approximation given by Eq. (4) is null when the specimen has a large  $E_x/G_{xy}$  value or a large  $H/L$  ratio.

## FE analysis (FEA)

The 2D FEA was performed prior to the vibration test based on ANSYS software version 6.0. Figure 1Ab shows the FE mesh of the specimen, which is homogeneously divided. The model dimensions are length  $L=200$  mm and width  $B=10$  mm. The height  $H$  is varied from 10 to 60 mm at intervals of 10 mm. The model consists of four-node plane elements. The mesh size was confirmed to be fine enough so that the effect of mesh size could be ignored.

The elastic properties required for the calculations are listed in Table 1. The MOEs in the L and R directions are designated as  $E_L$  and  $E_R$ , respectively, and the SM and Poisson's ratio in the LR plane are designated as  $G_{LR}$  and  $\nu_{LR}$ , respectively. These properties were taken from the data of Douglas fir (*Pseudotsuga menziesii*) reported by Hearmon (1948) (see Table 1).

Prior to the FEAs, the resonance frequencies corresponding to the first to fourth FV modes were calculated by substituting the  $E_L$ ,  $E_R$ , and  $G_{LR}$  values listed in Table 1 into Eqs. (1) and (4) by means of the goal seek function of Microsoft Excel version 14.4.1. The resonance frequencies calculated from this procedure were compared with those extracted in the FEAs.

Model scenarios for the FEAs: (a) the length direction coincides with the L direction (L-type model) and (b) the length direction coincides with the R direction (R-type model). The modal analyses were conducted, and the resonance frequencies from the first to fourth FV modes were extracted: the values of MOE and SM,  $E_x$  and  $G_{xy}$ , were determined from the following two procedures. (1) The  $E_x$  and  $G_{xy}$  terms were calculated from the solution to Eq. (1) using Excel. The  $G_{xy}$  values corresponding to each vibration mode were calculated by altering the value of  $E_x/G_{xy}$ , and then the coefficient of variation (COV) of the  $G_{xy}$  values was determined. The  $E_x/G_{xy}$  value that generates the minimum COV of the  $G_{xy}$  values and the mean value of  $G_{xy}$  can be regarded as being the most feasible. In previous studies, this calculation was conducted by Mathematica 6 (Yoshihara 2011, 2012a, b, c). However, the goal seek function incorporated in Excel is easier in handling. (2) The  $E_x$  and  $G_{xy}$  terms were calculated from the iteration in Eq. (7)

**Table 1** Elastic properties of Douglas fir according to Hearmon (1948) used for the FE calculations in the present study.

$\rho$ (kg m <sup>-3</sup> )	$E_L$ (GPa)	$E_R$ (GPa)	$G_{LR}$ (GPa)	$\nu_{LR}$
0.50	15.7	1.06	0.88	0.29

and the resonance of the first to fourth FV modes. Initially, a virtual value of  $G_{xy}$  was substituted into  $Y$  of Eq. (7), and the refined value of  $G_{xy}$  obtained as  $sq/p$  was again substituted into  $Y$  (Hearmon 1958). The iterative procedure was conducted by Excel. The procedure was halted after all the values in the formulas changed by  $<0.001$  between the iterations.

In addition to the FV analyses, the  $E_x$  value was also calculated by substituting the resonance frequency of first longitudinal vibration (LV) mode,  $f_L$ , into the following equation:

$$E_x = 4f_L^2 L^2 \rho \quad (8)$$

The  $E_x$  value obtained from the LV analysis was compared with those from the FV analyses. The  $E_x$  values obtained from the L- and R-type specimens are designated as  $E_L$  and  $E_R$ , respectively, and the  $G_{xy}$  values obtained from the L- and R-type specimens are designated as  $G_{LR}^L$  and  $G_{LR}^R$ , respectively.

## Materials and methods

The density at 12% moisture content (MC) of the investigated Douglas fir (*Pseudotsuga menziesii*) lumber was  $632 \pm 10 \text{ kg m}^{-3}$ . The samples contained four to five annual rings per 10 mm in the R direction; the rings were flat enough that their curvature could be ignored. This lumber was free of defects and knots or grain distortions, so the specimens cut from it could be regarded as “small and clear”. The lumber was stored at a constant  $20^\circ\text{C}$  and 65% relative humidity (RH) before the test, and the specimens were in an air-dried condition, which was kept throughout the tests. The equilibrium MC (EMC) condition was approximately 12%.

The lumber was sliced into multiple quarter-sawn boards, and the specimens were cut from the boards. Initially, 10 specimens with length $\times$ height $\times$ width of  $200 \times 60 \times 10 \text{ mm}^3$  were cut from the lumber shown in Figure 1B. After conducting the FV tests described below, the height ( $H$ ) of the specimen was decreased, and the succeeding series of vibration tests was conducted with the specimens with decreasing heights from 60 to 10 mm in intervals of 10 mm. The average densities were 632, 634, 632, 632, 630, and 632  $\text{kg m}^{-3}$  corresponding to the depth from 60 to 10 mm, respectively.

The specimen was suspended by threads at the nodal positions of the free-free resonance vibration mode  $f_n$  and excited in the depth ( $Y$ ) direction with a hammer (Figure 1Aa). Similar to several previous studies (Yoshihara 2011, 2012a, b, c), the first- to fourth-mode resonance frequencies were measured. The resonance frequencies were analyzed by a fast Fourier transform (FFT) analysis program. The  $E_x$  and  $G_{xy}$  values were calculated from Eqs. (1) and (7) by Excel version 14.4.1 (see above). Similar to the FEAs, the  $E_x$  values obtained from the L- and R-type specimens are designated as  $E_L$  and  $E_R$ , respectively, and the  $G_{xy}$  values obtained from the L- and R-type specimens are designated as  $G_{LR}^L$  and  $G_{LR}^R$ , respectively. For the R-type specimen with  $H=10$  and 20 mm, however, the  $E_x/G_{LR}^R$  value for the first

flexural resonance mode was often a negative or extremely large value because of the small deflection caused by the shearing force in the analysis by the rigorous solution. The inaccuracy of the  $E_x/G_{LR}^R$  value was also significant in the analysis by the approximated solution. Therefore, the data obtained from the first mode were not included in the analysis of the specimen with  $H=10$  and 20 mm.

In the LV tests, the specimen was supported by a soft foam at the mid-length and excited along the length direction with a hammer to obtain the  $f_L$  value. The  $E_x$  value, which coincides with the  $E_L$  and  $E_R$  values for the L- and R-type specimens, respectively, was calculated by substituting  $f_L$  into Eq. (8).

## Results and discussion

### FE analysis (FEA)

The resonance frequency obtained from the FEA is defined as  $f_n^{\text{FEA}}$  (based on the  $E_L$ ,  $E_R$ , and  $G_{LR}$  data in Table 1, according to Hearmon 1948), whereas that calculated by substituting the  $E_L$  and  $G_{LR}$  data into Eqs. (1) and (4) is defined as  $f_n^{\text{calc}}$ . Figure 2 shows the  $f_n^{\text{FEA}}/f_n^{\text{calc}}$  ratio corresponding to each FV mode. Note that the MOE and SM cannot be reproduced accurately from the calculation when the  $f_n^{\text{FEA}}/f_n^{\text{calc}}$  value deviates from 1. In the case of the rigorous solution [Eq. (1)], the deviation of the  $f_n^{\text{FEA}}/f_n^{\text{calc}}$  value is moderate, although it is rather significant in the fourth mode of the L-type model with the  $H/L$

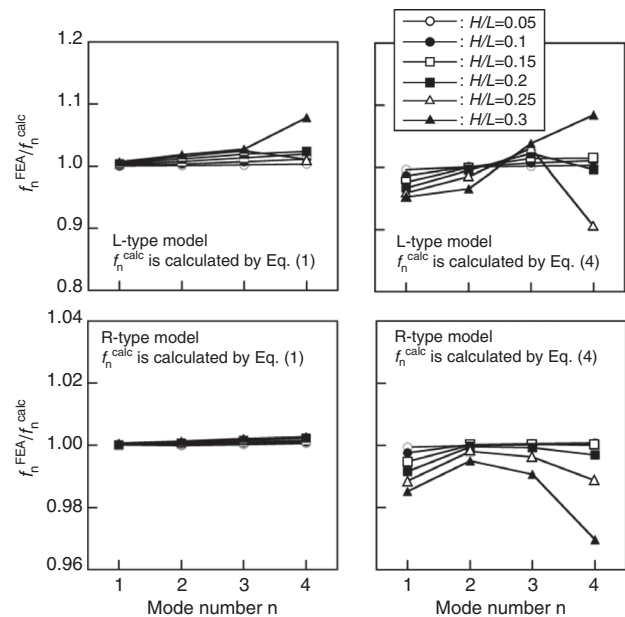


**Figure 2** Ratio of resonance frequency obtained from the FEA, defined as  $f_n^{\text{FEA}}$ , to that calculated by substituting the  $E_L$ ,  $E_R$ , and  $G_{LR}$  values listed in Table 1 into Eqs. (1) and (4), defined as  $f_n^{\text{calc}}$ , corresponding to each FV mode.

value of 0.3 ( $H=60$  mm). In contrast, in the case of the T-G solution [Eq. (4)], the deviation is significant. In particular, the deviation is enhanced when the  $H/L$  value exceeds 0.25 ( $H=50$  mm) in the fourth mode for both models. This observation confirms the hypothesis of this work that the MOE and SM cannot be accurate in the case of specimens with  $H/L > 0.25$ .

Figure 3 shows the MOEs in the L and R directions,  $E_L$  and  $E_R$ , respectively, and the SMs in the LR plane of the L- and R-type models,  $G_{LR}^L$  and  $G_{LR}^R$ , respectively, obtained by FEA with different  $H/L$  ratios. The  $E_L$  values obtained from the rigorous solution and LV, which correspond to Eqs. (1) and (8), respectively, coincide well with the MOE input in the program ( $=15.7$  GPa). Nevertheless, the  $E_L$  value obtained from the iteration based on the approximated solution [Eq. (7)] markedly decreases when the  $H/L$  value is larger than 0.25. In contrast, the variation of the  $E_R$  value against the  $H/L$  is smaller than that of the  $E_L$  values obtained from the approximated solution. In the case of the rigorous solution, the  $G_{LR}^L$  and  $G_{LR}^R$  values are close to the SM input in the program ( $=0.88$  GPa), except for the  $G_{LR}^L$  value at  $H/L=0.3$ , which is slightly larger than 0.88 GPa. When using the approximate solution, the  $G_{LR}^L$  value is markedly large if  $H/L=0.3$  ( $H=60$  mm). Although the  $G_{LR}^R$  value gradually decreases all over the  $H/L$  range, it is markedly smaller than the input value if  $H/L > 0.25$

( $H=50$  mm). The MOE and SM values obtained from the FEA also confirm the doubts about the less reliable results in the case of  $H/L > 0.25$ .

## FV and LV tests

Figure 4 shows the dependence of the  $E_L$ ,  $E_R$ ,  $G_{LR}^L$ , and  $G_{LR}^R$  values obtained from the actual FV and LV tests on the  $H/L$  value and COVs corresponding to each property. Similar to the FEA results, the  $E_L$  value obtained from Eq. (7) markedly decreases when  $H/L > 0.25$ . The statistical analysis of the difference between the  $E_L$  values obtained from the approximate solution [Eq. (7)] and the LV test [Eq. (8)] indicates that the difference is significant for the  $H/L$  values of 0.25 and 0.3. In contrast, the difference between the  $E_L$  values obtained from the rigorous solution [Eq. (1)] and Eq. (8) was not significant.

For the  $E_R$  values, there is a significant difference between the values obtained from the approximate solution and the LV test when the  $H/L=0.3$  at the significance level of 0.01. Except for this occasion, the influence of the equation used for the analysis was not significant.

The statistical analysis indicates that the  $G_{LR}^L$  values for the  $H/L$  value of 0.3 are significantly larger than those for  $H/L < 0.25$  and that this tendency is the same for both

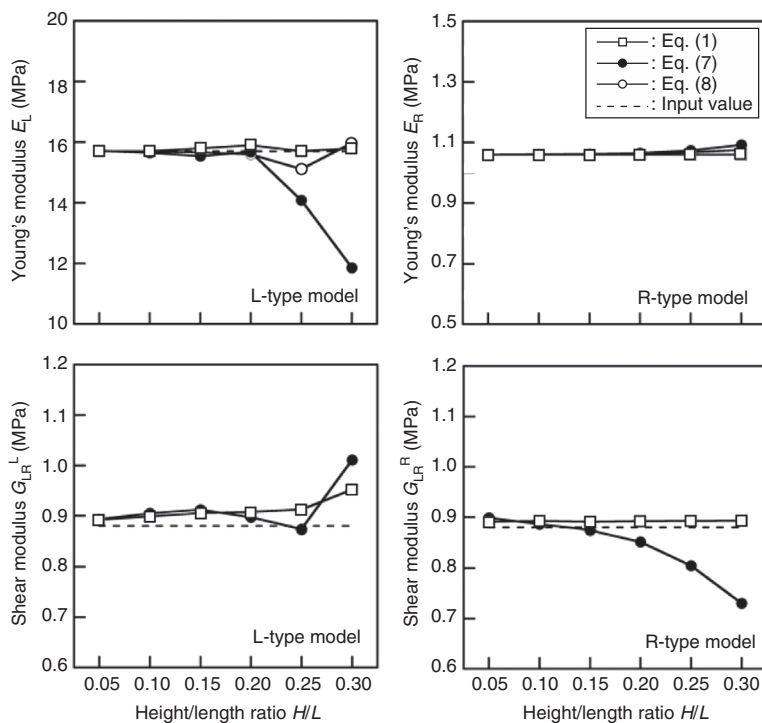


**Figure 3** MOEs in the L and R directions,  $E_L$  and  $E_R$ , respectively, and SM in the LR plane of the L- and R-type models,  $G_{LR}^L$  and  $G_{LR}^R$ , respectively, obtained by FEA corresponding to the  $H/L$  ratios.

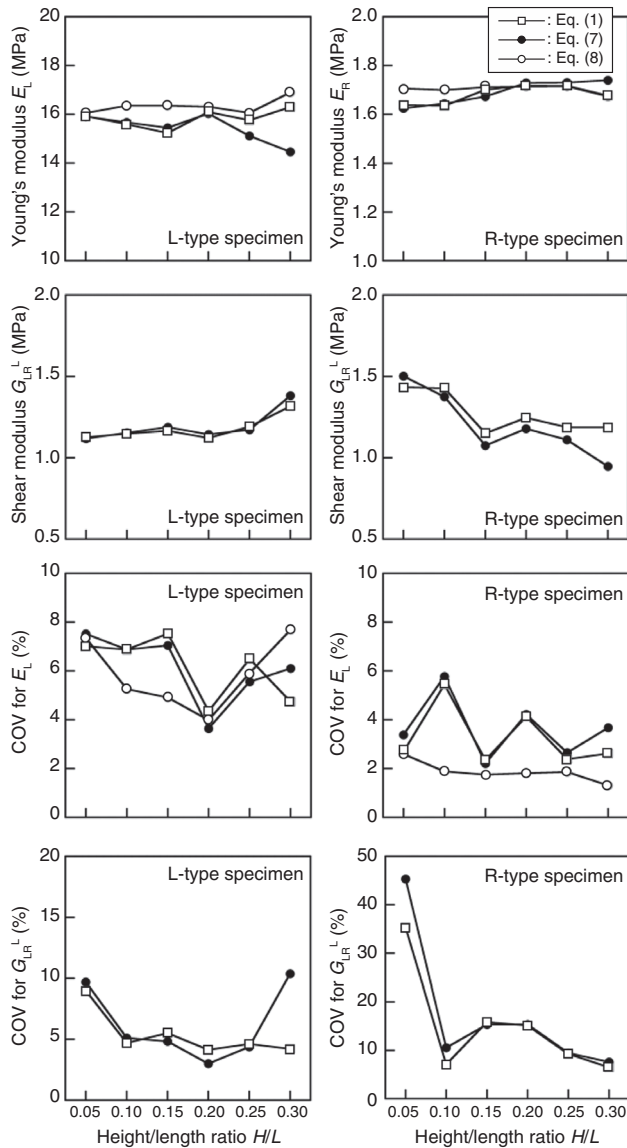


**Figure 4** Dependence of the  $E_L$ ,  $E_R$ ,  $G_{LR}^L$ , and  $G_{LR}^R$  values experimentally obtained on the  $H/L$  values and COVs corresponding to each property.

the rigorous and approximated solutions. Except for this condition, the difference between the  $G_{LR}^L$  values is not significant, so that the  $G_{LR}^L$  value can be obtained accurately.

The  $G_{LR}^R$  values for  $H/L$  of 0.05 ( $H=10$  mm) and 0.1 ( $H=20$  mm) are significantly larger than those for the  $H/L>0.15$  ( $H=30$  mm). As described above, the resonance frequency of the first FV mode was not included in the analysis of the specimen with  $H/L=0.05$  and 0.1. Even when the data of the first resonance mode is reduced, it is still difficult to measure the  $G_{LR}^R$  accurately in this  $H/L$  range because the deflection caused by the shearing force is significantly

smaller than that caused by the bending moment for the higher resonance modes. The large COV value at  $H/L=0.1$  also indicates the difficulty in measuring the  $G_{LR}^R$  accurately when the specimen is too slender. The MOE and SM values obtained from the FEA confirm the problems in the case of  $H/L>0.25$ . Except for these  $H/L$  values, the  $G_{LR}^R$  obtained by the rigorous solution is accurate. The approximate solution, however, delivers the  $G_{LR}^R$  data for  $H/L=0.3$ , which are markedly smaller than those for  $H/L<0.25$ .

## Conclusions

The MOE in the L and R directions and the SM in the LR plane of Douglas fir were measured by FV tests of the specimen, the  $H/L$  ratio of which was in the range of 0.05–0.3, and the validity of the MOE and SM values was examined through a subsequent numerical analysis. The range of the  $H/L$  value of the specimens should be restricted in the case of an accurate MOE and SM determination by means of the approximate solution. The experimental results indicated that the  $H/L$  of the specimens should be smaller than 0.2 and 0.25 for measuring the  $E_L$ ,  $E_R$ , and  $G_{LR}^L$  values, respectively. In contrast, the  $H/L$  should be restricted in the range of 0.15–0.25 for measuring the  $G_{LR}^R$  value. Otherwise, the rigorous solution should be used regardless of its more complicated application and longer calculation times.

**Acknowledgments:** This work was supported in part by a Grant-in-Aid for Scientific Research (C) (No. 24580246) of the Japan Society for the Promotion of Science.

## References

- Brancheriau, L. (2006) Influence of cross section dimensions on Timoshenko's shear factor. Application to wooden beams in free-free flexural vibration. *Ann. For. Sci.* 63:319–312.
- Brancheriau, L., Baillères, H. (2002) Natural vibration analysis of clear wooden beams: a theoretical review. *Wood Sci. Technol.* 36:347–365.
- Brancheriau, L., Baillères, H. (2003) Use of the partial least squares method with acoustic vibration spectra as a new grading technique for structural timber. *Holzforschung* 57:644–652.
- Chui, Y.H., Smith, I. (1990) Influence of rotatory inertia, shear deformation and support condition on natural frequencies of wooden beams. *Wood Sci. Technol.* 24:233–245.
- Divós, F., Tanaka, T., Nagao, H., Kato, H. (1998) Determination of shear modulus on construction size timber. *Wood Sci. Technol.* 32:393–402.
- Divós, F., Denes, L., Iñigues, G. (2005) Effect of cross-sectional change of a board specimen on stress wave velocity determination. *Holzforschung* 59:230–231.

- Goens, E. (1931) Über die Bestimmung des Elastizitätsmodulus von Stäben mit Hilfe von Biegungsschwingungen. *Ann. Physik. Ser.* 7 11:649–678.
- Hearmon, R.F.S. *Elasticity of Wood and Plywood*. His Majesty Stationary Office, London, 1948.
- Hearmon, R.F.S. (1958) The influence of shear and rotatory inertia on the free flexural vibration of wooden beams. *Br. J. Appl. Phys.* 9:381–388.
- Hearmon, R.F.S. (1966) Vibration testing of wood. *For. Prod. J.* 16:29–40.
- Kubojima, Y., Tonosaki, M. (2013) Effect of specimen width on shear modulus of wood obtained by flexural vibration tests. *Wood Fiber Sci.* 45:170–177.
- Kubojima, Y., Yoshihara, H., Ohta, M., Okano, T. (1996) Examination of the method of measuring the shear modulus of wood based on the Timoshenko theory of bending. *Mokuzai Gakkaishi* 42:1170–1176.
- Kubojima, Y., Yoshihara, H., Ohta, M., Okano, T. (1997) Accuracy of the shear modulus of wood obtained by the Timoshenko's theory of bending. *Mokuzai Gakkaishi* 43:439–443.
- Mead, D.J., Joannides, R.J. (1991) Measurement of the dynamic moduli and Poisson's ratios of a transversely isotropic fibre-reinforced plastic. *Composites* 22:15–29.
- Murata, K., Kanazawa, T. (2007) Determination of Young's modulus and shear modulus by means of deflection curves for wood beams obtained in static bending tests. *Holzforschung* 61:589–594.
- Nakao, T. (1984) Measurement of the anisotropic-shear modulus by the torsional vibration method for free-free wooden beams. *Mokuzai Gakkaishi* 30:877–885.
- Ono, T. (1983) Effect of grain angle on dynamic mechanical properties of wood. *J. Mater. Res. Soc. Jpn.* 32:108–113.
- Ono, T., Kataoka, A. (1979a) The frequency dependence of the dynamic Young's modulus and internal friction of wood used for the soundboards of musical instruments I. Effect of rotatory inertia and shear on the flexural vibration of free-free beams. *Mokuzai Gakkaishi* 25:461–468.
- Ono, T., Kataoka, A. (1979b) The frequency dependence of the dynamic Young's modulus and internal friction of wood used for the soundboards of musical instruments II. The dependence of the Young's modulus and internal friction on frequency, and the mechanical frequency dispersion. *Mokuzai Gakkaishi* 25:535–542.
- Sobue, N. (1986) Instantaneous measurement of elastic constants by analysis of the tap tone of wood: application to flexural vibration of beams. *Mokuzai Gakkaishi* 32:274–279.
- Sohi, A.M.A., Khademi-Eslam, H., Hemmasi, A.H., Roohnia, M., Talaipour, M. (2011) Nondestructive detection of the effect of drilling of acoustic performance of wood. *BioResources* 6:2632–2646.
- Timoshenko, S.P. (1921) On the correction for shear of the differential equation for transverse vibrations of prismatic bars. *Phil. Mag.* 41:744–746.
- Tonosaki, M., Saito, S., Miyamoto, K. (2010) Evaluation of internal checks in high temperature dried Sugi boxed heart square sawn timber by dynamic shear modulus. *Mokuzai Gakkaishi* 56:79–83.
- Yoshihara, H. (2011) Measurement of the Young's modulus and shear modulus of in-plane quasi-isotropic medium-density fiberboard by flexural vibration. *BioResources* 6:4871–4885.
- Yoshihara, H. (2012a) Off-axis Young's modulus and off-axis shear modulus of wood measured by flexural vibration tests. *Holz-forschung* 66:207–213.
- Yoshihara, H. (2012b) Examination of the specimen configuration and analysis method in the flexural vibration test of solid wood and wood-based materials. *For. Prod. J.* 62:191–200.
- Yoshihara, H. (2012c) Influence of the specimen depth to length ratio and lamination construction on Young's modulus and in-plane shear modulus of plywood measured by flexural vibration. *BioResources* 7:1337–1351.